The EMBO Journal Vol.17 No.1 pp.50–60, 1998

A systematic survey of conserved histidines in the core subunits of Photosystem I by site-directed mutagenesis reveals the likely axial ligands of P_{700}

Kevin Redding, Fraser MacMillan[1], Winfried Leibl[1], Klaus Brettel[1], Jonathan Hanley[1], A.William Rutherford[1], Jacques Breton[1] and Jean-David Rochaix[2]

Departments of Molecular and Plant Biology, University of Geneva, 30, quai Ernest-Ansermet, CH-1211 Geneva 4, Switzerland and [1]Section de Bioénergétique CNRS URA 2096, DCBM, CEA Saclay, Bâtiment 532, Gif-sur-Yvette Cedex 91191, France

[2]Corresponding author

The Photosystem I complex catalyses the transfer of an electron from lumenal plastocyanin to stromal ferredoxin, using the energy of an absorbed photon. The initial photochemical event is the transfer of an electron from the excited state of P_{700}, a pair of chlorophylls, to a monomer chlorophyll serving as the primary electron acceptor. We have performed a systematic survey of conserved histidines in the last six transmembrane segments of the related polytopic membrane proteins PsaA and PsaB in the green alga *Chlamydomonas reinhardtii*. These histidines, which are present in analogous positions in both proteins, were changed to glutamine or leucine by site-directed mutagenesis. Double mutants in which both histidines had been changed to glutamine were screened for changes in the characteristics of P_{700} using electron paramagnetic resonance, Fourier transform infrared and visible spectroscopy. Only mutations in the histidines of helix 10 (PsaA-His676 and PsaB-His656) resulted in changes in spectroscopic properties of P_{700}, leading us to conclude that these histidines are most likely the axial ligands to the P_{700} chlorophylls.

Keywords: *Chlamydomonas reinhardtii*/EPR/FTIR/photosystem I/site-directed mutagenesis

Introduction

Photosystem I (PS1) is an integral membrane, multisubunit complex that uses light energy to drive electrons both across the thylakoid membrane from the lumenal to the stromal side and up an energy barrier of >700 mV between the soluble electron carriers plastocyanin and ferredoxin (for recent reviews, see Golbeck and Bryant, 1991; Chitnis, 1996; Brettel, 1997). PS1 is present in all oxygenic photosynthetic organisms along with photosystem II (PS2). It is required for efficient generation of low-potential reductants, and can function in linear electron transport in concert with PS2 and cytochrome b_6f to generate NADPH and a proton gradient or in a cyclic mode with cytochrome b_6f to generate a proton gradient (Bendall and Manasse, 1995), which is used by the chloroplast ATP synthase to produce ATP (Boyer, 1993).

The core of PS1 consists of two integral membrane proteins, PsaA and PsaB. These proteins are related to each other, sharing 45–50% identical residues and each containing 11 transmembrane α-helices (Fish *et al.*, 1985; Vallon and Bogorad, 1993). The X-ray crystal structure of PS1 reveals that the helices of the C-terminal half of these proteins together form a cage holding the cofactors involved in electron transfer from the lumenal to stromal compartments (Krauss *et al.*, 1996). In order, they are: P_{700}, a pair of chlorophyll *a* (Chl *a*) molecules; A_0, a Chl *a*; A_1, a phylloquinone; and F_X, a 4Fe–4S iron–sulfur cluster. The terminal electron acceptors, F_A and F_B, which are also 4Fe–4S clusters, are bound by the small, extrinsic subunit PsaC on the stromal side. After excitation of P_{700}, an electron is transferred to A_0, and subsequently to A_1, through the iron–sulfur clusters, and finally to a reversibly bound ferredoxin, whose docking is facilitated by the extrinsic proteins PsaD and PsaE (Xu *et al.*, 1994). Likewise, PsaF in green plants plays a role in the docking of reversibly bound plastocyanin (or cytochrome *c*), which reduces P_{700}^+ (Farah *et al.*, 1995; Hippler *et al.*, 1997). PS1 belongs to the family of type 1 reaction centres (RCs) that use iron–sulfur centres as terminal electron acceptors. This family includes the RCs of green sulfur bacteria (e.g. *Chlorobium*) and Heliobacteriaceae (Büttner *et al.*, 1992a; Liebl *et al.*, 1993). However, the core of PS1 is reminiscent of the purple bacterial RC, a member of the type 2 family, which uses quinones as the terminal electron acceptors. The purple bacterial RC, whose structure has been solved to 2.3 Å resolution (Deisenhofer *et al.*, 1995), consists of two related membrane proteins, L and M, each of which has five transmembrane helices. The pigments are arranged in two symmetrical branches, starting from the dimeric 'special pair' of bacteriochlorophylls (BChls) through the accessory BChls, pheophytins (analogous in their position to A_0 of PS1) and quinones.

Chlamydomonas reinhardtii has served as a very useful model organism for genetic and biochemical/biophysical analysis of photosynthesis (Rochaix, 1995). As this eukaryotic green alga can grow well in the absence of photosynthetic functions on media supplemented with acetate (Harris, 1989), it is ideal for structure/function analysis of photosynthetic proteins. The chloroplast in *C.reinhardtii* is a single, cup-shaped organelle which has its own genome of 196 kilobase pairs present at 80–100 copies per cell. The advent of chloroplast genome transformation and selectable markers has enabled site-directed mutagenesis of chloroplast genome-encoded proteins (Boynton *et al.*, 1988; Goldschmidt-Clermont, 1991). The genes encoding the three cofactor-bearing subunits of PS1 (PsaA, PsaB and PsaC) have been inactivated, resulting in the loss of the PS1 complex and photosynthetic growth (Takahashi *et al.*, 1991; Fischer *et al.*, 1996; this work).

Several mutations have been generated in the PsaA and PsaB proteins. On the acceptor side, mutations have been generated that affect the F_X iron–sulfur centre (Webber *et al.*, 1993; Hallahan *et al.*, 1995), and association with the PsaC subunit (Rodday *et al.*, 1995). The fact that helix 8, directly before the stromal loop involved in ligating F_X, has two conserved histidines led to the suggestion that these might coordinate the chlorophylls of P_{700} or A_0 (Büttner *et al.*, 1992b; Liebl *et al.*, 1993). However, although mutations of the helix 8 histidines in PsaB decreased accumulation of PS1, they had no effect upon spectroscopic properties of P_{700} (Cui *et al.*, 1995). Attention has been focused on helix 10, where there is a single conserved histidine. The PsaB-H656N mutation exhibited several effects upon P_{700}: a noticeably changed visible difference spectrum ($P_{700}^+ - P_{700}$), a 40 mV increase in the redox potential of the P_{700}/P_{700}^+ couple, and a modified electron nuclear double resonance (ENDOR) spectrum of P_{700}^+ (Webber *et al.*, 1996). Ultra-fast absorption spectroscopy analysis demonstrated that the PsaB-H656N mutation affects the $P_{700}^+ - P_{700}$ difference spectrum, but not the $A_0^- - A_0$ difference spectrum, suggesting that the mutation has a localized effect (Melkozernov *et al.*, 1997). These experiments, along with fluorescence decay analysis, indicate that the intrinsic rate of charge separation has been decreased by the mutation.

Histidines are often ligands to cofactors such as Chl, quinones and metal ions. We identified nine sites in the last six transmembrane helices of PsaA and PsaB that are always occupied by histidines in both proteins (see Figure 1A). Thus, they should occupy symmetrical positions in the PsaA/PsaB heterodimer, since there are two quasi-symmetric branches seen in the crystal structure of PS1 (Krauss *et al.*, 1996). We decided to target these histidines by site-directed mutagenesis, in order to identify those that interact with the primary donor, P_{700}. As the histidines in helix 8 had already been mutated in PsaB by Cui *et al.* (1995) with no effects upon P_{700}, we did not include these in our study. The remaining histidines at these sites in both PsaA and PsaB were changed to glutamine and, in some cases, leucine. We constructed double mutations such that the same site was mutated in both PsaA and PsaB, which allowed us to screen more efficiently through the collection of mutations. A biochemical and biophysical analysis of the double mutants allowed us to conclude that only the histidines in helix 10 interact with P_{700} in any significant way.

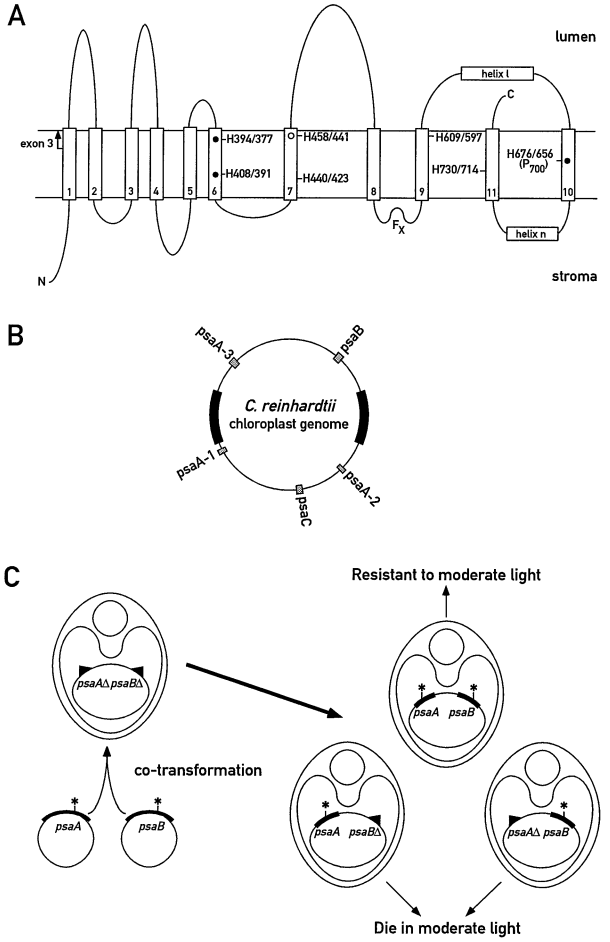

Fig. 1. Strategy for site-directed mutagenesis. (**A**) The mutation sites are mapped onto the corresponding region of the PsaA and PsaB proteins using the topological model of Krauss *et al.* (1996). The vertical bars represent transmembrane helices and are numbered from 1 to 11 (Fish *et al.*, 1985). The two horizontal bars represent the parallel α-helices termed 'n' and 'l' found in the crystal structure (Krauss *et al.*, 1996). The histidines are numbered according to the *C.reinhardtii* sequence (Kück *et al.*, 1987; the error in the numbering of PsaA residues has been corrected here), with PsaA first and PsaB second. The start point of *psaA* exon 3 is indicated with an arrow. Histidines that are conserved between *Chlorobium* PscA (Büttner *et al.*, 1992a) and *Heliobacillus* PshA (Liebl *et al.*, 1993) are shown as dark circles, and by open circles for those conserved with *Heliobacillus* PshA only. Additionally, the lumenal and stromal sides of the thylakoid membrane are marked, as well as the region involved in binding the F_X iron–sulfur centre. (**B**) Map of the chloroplast genome indicating the genes encoding the core subunits of PS1, including all three of the *psaA* exons. Black bars indicate the inverted repeat. (**C**) Double mutant selection strategy. Upon co-transformation of the *psaA-3*Δ *psaB*Δ double mutant with plasmids containing mutations at the same site in *psaA* and *psaB*, selection for spectinomycin resistance will give single and double transformants. The latter are selected for by moderate illumination, which inhibits the growth of $PS1^-$ mutants. Bars indicate genes, triangles represent deletions and asterisks represent point mutations.

Results

Mutagenesis strategy

Previously, we described a method to delete genes in the chloroplast genome with subsequent loss of the bacterial gene *aadA* used as an antibiotic resistance marker (Goldschmidt-Clermont, 1991; Fischer *et al.*, 1996). We took advantage of strains that lack the *psaA-3* and *psaB* genes to reintroduce the mutant genes. This allows for rapid creation of mutant strains, as we are not forced to wait until every copy of the 80–100 copies of the chloroplast genome has been replaced by the newly introduced gene (Newman *et al.*, 1991). The vectors have been designed such that the *aadA* cassette, which is used to select for transformation, is placed within a nearby piece of flanking DNA which was deleted in the null mutants, thus eliminating the possibility of recombination between the *aadA* gene and the point mutation. Additionally, we have placed unique restriction sites throughout each gene such that we can easily introduce point mutations at any position using a simple one-tube PCR reaction (Picard *et al.*, 1994). Mutagenesis of *psaA* is slightly complicated by the fact that this gene is split into three exons that are

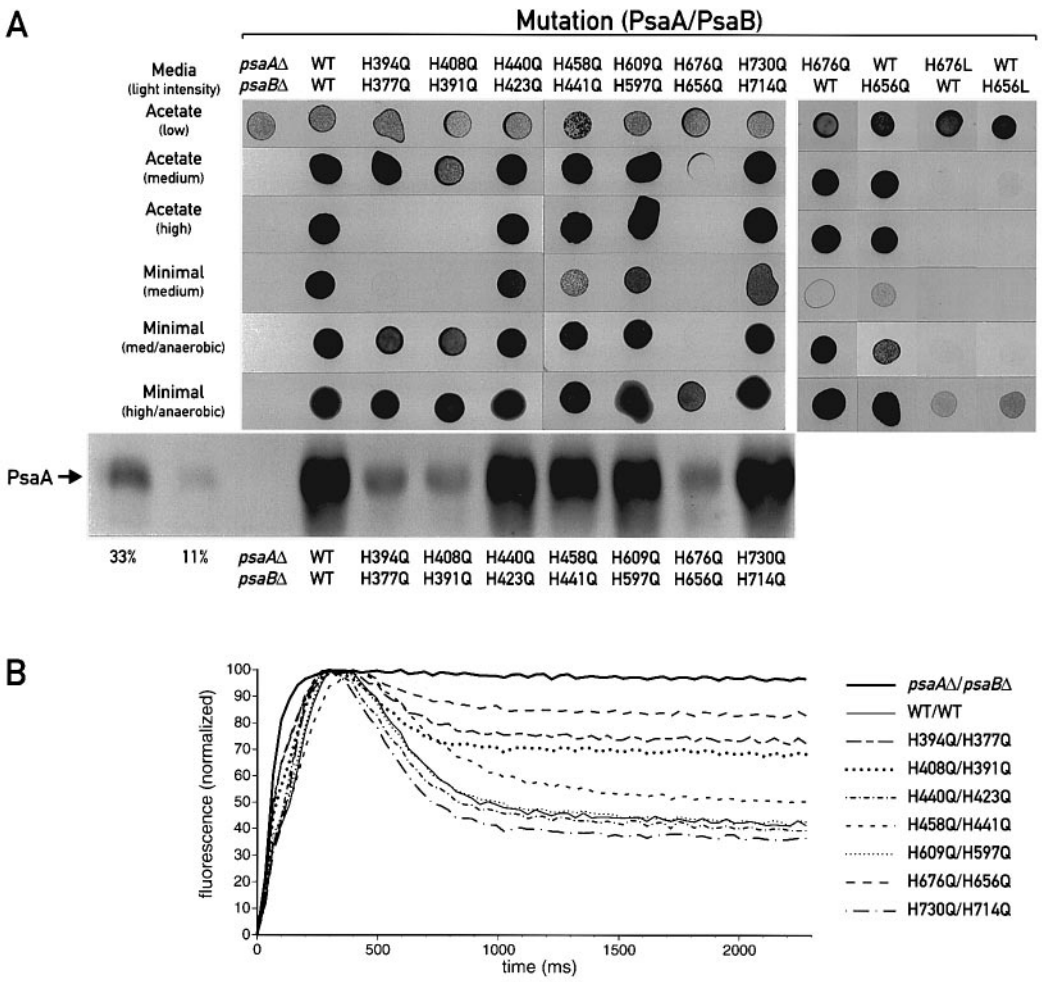

Fig. 2. *In vivo* characteristics of double mutants. The indicated strains were grown in liquid culture in acetate-containing medium under low illumination (<1 μEinstein/m^2/s) before spotting onto agar plates. A portion of each culture was also harvested for immunoblot analysis. (**A**) Results of growth tests under various conditions and immunoblot analysis of PS1 from each strain. The identity of each strain is indicated at the top. 'Acetate' refers to TAP medium. Minimal medium demands photosynthetic growth. The light fluences are indicated in parentheses: low (0.5 μEinstein/m^2/s); medium (50 μEinstein/m^2/s); and high (500 μEinstein/m^2/s). The bottom row is the result of an immunoblot using a polyclonal antiserum raised against the N-terminus of PsaA. Each lane was loaded with 30 μg of total membrane protein. The lanes marked '33%' and '11%' represent serial 3-fold dilutions of the WT extract into the *psaAΔ/psaB*Δ extract and allow quantitation of PsaA abundance. (**B**) Fluorescence transients of the mutant strains. Cells grown in TAP (low light) were subjected to constant excitation (150 μEinstein/m^2/s of blue light) for 3 s and the resulting fluorescence was measured with a video imaging system. The values were normalized such that 0 corresponds to the initial fluorescence level and 100 corresponds to the maximal level for each curve.

trans-spliced together (Kück *et al.*, 1987; Choquet *et al.*, 1988; see Figure 1B for locations of the exons in the chloroplast genome). However, as the third exon (*psaA-3*) encodes the last 660 residues of PsaA (see Figure 1A), we may restrict ourselves to this exon for all the mutations described in this work.

The histidines that have been targeted are shown in Figure 1A. Each histidine was changed individually to glutamine and leucine. Two independent clones were used to transform null mutants to ensure that any observed phenotypes were due to the point mutation and not to other mutations inadvertently introduced elsewhere. We also created double mutants such that both histidines in homologous positions in PsaA and PsaB were changed to glutamine (or leucine) by cotransforming the respective mutant *psaA-3* and *psaB* vectors into a strain lacking both *psaA-3* and *psaB*. As both vectors contain the *aadA* gene, selection for spectinomycin resistance does not select for double transformants, but single transformants are PS1$^-$ due to the lack of the other gene. As PS1-deficient mutants are light-sensitive (Spreitzer and Mets, 1981; see Figure 2A), the double transformants can be selected by passage on acetate-containing medium under weak to moderate illumination. This method assumes that the double mutant PS1 will provide enough activity that it can be distinguished from a PS1 null mutant. This proved to be the case for all the double glutamine substitution (double-Gln) mutants, but some of the double leucine substitution mutants were impossible to obtain. In the interests of brevity, we will refer to the PsaA-H394Q/PsaB-H377Q double substitution mutant as 'H394Q/H377Q', and the others likewise.

For the biochemical and biophysical analyses, we constructed PS2-less versions of all these mutants. The genes for *psaA* or *psaB* were deleted in the FUD7 mutant, which has a large deletion in the *psbA* gene encoding the D1 subunit of PS2 (Bennoun *et al.*, 1986), and these PS2$^-$/PS1$^-$ mutants were used to reintroduce mutant PS1 genes

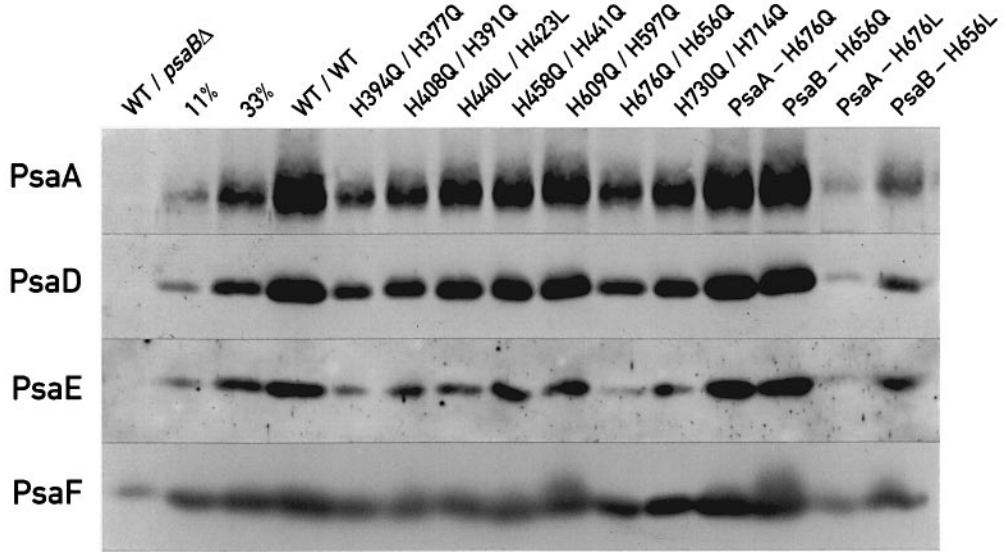

Fig. 3. Western analysis of thylakoids from PS1 mutants. Thylakoid membranes were prepared from PS2-less strains (*nac2* for double substitution mutants and FUD7 for single substitution mutants) and dissolved with SDS. Two μg of Chl was loaded onto each lane, and the blots were probed with antibodies against the indicated subunits (PsaA, PsaD, PsaE and PsaF). The genotypes are indicated above the lanes, with *psaA* preceding *psaB*. No detectable PsaA, PsaD or PsaE, and only small amounts of PsaF accumulate in thylakoids from the *psaB*Δ mutant. The lanes marked '33%' and '11%' represent serial 3-fold dilutions of the WT extract into the *psaB*Δ extract and facilitate quantitation of the abundance of each subunit.

as described above. As this method is not possible for the double mutants, they were crossed to a *nac2* mutant, which fails to express the D2 subunit of PS2 (Kuchka *et al.*, 1989), to obtain *nac2* segregants harbouring the two PS1 mutations.

In vivo characterization

The *in vivo* characterization of the double-Gln mutants is shown in Figure 2. All the strains grew well on acetate-containing medium in low light, indicating that they had no general growth defects (Figure 2A). However, the PS1$^-$ null mutants fail to grow upon illumination at light levels considered normal for growth of wild-type (WT) *C.reinhardtii* (50 μEinstein/m^2/s) due to the light sensitivity of PS1$^-$ mutants (Spreitzer and Mets, 1981). Under the same light intensities on minimal medium, the situation is even more demanding, with PS1 activity required for both photosynthesis and light resistance. Recently, we have discovered that the observed light sensitivity of PS1$^-$ mutants requires the presence of oxygen (Fischer *et al.*, 1997; K.Redding, M.Hippler, N.Fischer and J.-D.Rochaix, unpublished results). Thus, growth on minimal medium in anaerobic conditions allows the separate examination of these two *in vivo* functions of PS1.

Variations in the ability to grow photosynthetically can be explained for the most part by the level of PS1 abundance. Both double-Gln mutants in helix 6 (H394Q/H377Q and H408Q/H391Q) cause a 75–80% decrease in the amount of PS1 (Figure 2A, bottom row). Although the double-Gln mutant in helix 10 (H676Q/H656Q) is amassed at roughly this same level or higher, it clearly exhibits a stronger effect upon PS1 function. For example, both H394Q/H377Q and H408Q/H391Q are able to grow well anaerobically on minimal medium under normal illumination, while H676Q/H656Q grows quite poorly under these conditions (Figure 2A, fifth row). However, H676Q/H656Q grows much better when the light flux is increased 10-fold (Figure 2A, sixth row), indicating that PS1 function has become limiting for photosynthesis in this mutant, and that this limitation can be overcome by increasing the excitation of the mutant PS1. None of the double mutations in helices 7, 9 or 11 caused a dramatic *in vivo* phenotype, although H458Q/H441Q displayed a slight effect, which is difficult to explain by the fact that its accumulation is hardly reduced (Figure 2).

The kinetics of fluorescence induction in the double mutants after growth on acetate medium in low light are shown in Figure 2B. The initial increase in fluorescence, which arises mainly from the antenna of PS2, is due to the reduction of the plastoquinone pool by PS2 during the first few hundred milliseconds of illumination (Garnier *et al.*, 1979). The subsequent drop in fluorescence from the maximal level requires the action of PS1 and cytochrome b_6f (Chua and Bennoun, 1975), as they reoxidize the plastoquinone pool. Thus, the speed and extent of this drop in fluorescence can be taken as a relative measure of the functional capacity of PS1 *in vivo* (Bennoun and Chua, 1976). While the WT strain exhibited a large drop (50–60% of the variable fluorescence) from the maximal level within 500–600 ms, the fluorescence from the null mutant did not fall significantly during the first few seconds. The extent and speed of the fluorescence drop observed in all of the double mutants fell between these two extremes, and their order correlated with the degree of photosynthetic function seen in the growth tests.

The fact that the helix 10 double-Gln mutant seemed to be especially affected in photosynthetic function prompted us to examine the *in vivo* characteristics of the single glutamine and leucine substitution mutants in helix 10. As shown in Figure 2A, the single glutamine mutants grow much better than the double-Gln mutant, but the single leucine substitution mutants are even more severely affected. They are barely distinguishable from the null mutants in terms of light sensitivity, but their limited growth on minimal medium under anaerobic conditions

and intense illumination demonstrates that they are capable of reducing ferredoxin at an appreciable rate *in vivo*.

Biochemical characterization

After crossing the double mutants to a *nac2-26* mutant, we obtained $PS2^-$ segregants. Thylakoid membranes were prepared from these PS2-deficient cells for biochemical and biophysical analysis. In all cases we used the double-Gln mutants, the sole exception being H440L/H423L, which behaved identically to H440Q/H423Q in growth tests (data not shown).

Figure 3 presents immunoblots using these membranes and antibodies directed against various PS1 subunits. The lowered accumulation of PS1 in the helix 6 and helix 10 double mutants is similar to that observed in crude membranes from $PS2^+$ cells (Figures 2A and 3). A comparison of the signals obtained from the anti-PsaA antibody with those from antibodies against the stromal subunits PsaD and PsaE or the lumenal plastocyanin-docking PsaF subunit indicates that all seven of the PS1 double mutants accumulate these subunits. The PsaF subunit accumulates at a low level in thylakoids of the *psaB*Δ mutant, consistent with its identity as an integral membrane protein (Kruip *et al.*, 1997), while presence of the extrinsic PsaD and PsaE subunits requires assembly of PS1. This is due to the fact that most subunits of the multisubunit, membrane complexes of the thylakoid are degraded in the absence of a core subunit (Rochaix, 1992). Similar results were obtained with an antibody directed against PsaC (data not shown). Thus, any observed phenotypes of the double mutants cannot be attributed to the loss of other PS1 subunits.

All of the thylakoid membranes were assayed for PS1-mediated electron transport using 2,6-dichlorophenol indophenol and methyl viologen as electron donor and acceptor, respectively. For the most part, the rate of electron transport was proportional to the amount of PS1 determined by immunoblotting (Table I). However, the PsaA-H676L and PsaB-H656L mutants appeared to have ~40–50% of the expected activity.

Table I. Electron transport rates in thylakoid membranes from WT and PS1 mutants

Mutation[a]	O_2 uptake rate (% of WT)[b]	Amount of PS1 (% of WT)[c]
WT (*nac2*)	100 ± 7.6	100
*psaB*Δ (FUD7)	0.03 ± 1	0
H394Q/H377Q	24 ± 1.6	20 ± 3.5
H408Q/H391Q	25 ± 0.3	27 ± 4.6
H440L/H423L	34 ± 1.1	45 ± 4.2
H458Q/H441Q	31 ± 0.4	42 ± 3.7
H609Q/H597Q	40 ± 1.4	60 ± 4.9
H676Q/H656Q	26 ± 0.9	28 ± 2.2
H730Q/H714Q	51 ± 2	43 ± 4.4
PsaA-H676Q	65 ± 6.3	99 ± 1.9
PsaB-H656Q	89 ± 5.5	102 ± 3.0
PsaA-H676L	4.0 ± 0.1	8.9 ± 0.9
PsaB-H656L	12 ± 0.8	24 ± 0.4

[a]The thylakoid membranes shown in this table lacked PS2 due to the *nac2* mutation (double mutants) or to the FUD7 mutation (single mutants). They are the same as those used in Figures 3–6.
[b]O_2 uptake experiments were performed with an oxygen electrode in the presence of methyl viologen as electron acceptor and ascorbate/2,6-dichlorophenol indophenol as electron donor/mediator in darkness and saturating light. Light-dependent O_2 uptake activities are expressed relative to the WT (*nac2*) value, which was 60 ± 4.6 μmol O_2/mg Chl/h.
[c]The abundance of the PsaA and PsaD subunits relative to total Chl in each membrane preparation was quantified by densitometry of several immunoblots similar to that shown in Figure 3.

Table II. EPR linewidths of P_{700}^+ in WT and mutant PS1 thylakoid membranes

Sample[a]	ΔH_{pp} (mT)[c]	Sample[b]	ΔH_{pp} (mT)[c]
WT (*nac2*)	0.77	WT (FUD7)	0.77
H394Q/H377Q	0.76	PsaA-H676Q	0.76
H408Q/H391Q	0.76	PsaB-H656Q	0.83
H440L/H423L	0.76	PsaA-H676L	0.87
H458Q/H441Q	0.76	PsaB-H656L	0.88
H609Q/H597Q	0.76		
H676Q/H656Q	0.86	PsaB-H597L	0.75
H730Q/H714Q	0.77	PsaB-H714L	0.76
		PsaB-H714Q	0.75
WT PS1 particles[d]	0.76		

[a]All of the double substitution mutants were prepared from *nac2* cells.
[b]All of the single substitution mutants were prepared from FUD7 cells.
[c]The error in linewidths is ±0.01 mT.
[d]WT PS1 particles from a PS2-containing strain. (Thylakoids from this strain contained contributions from the PS2-Y_D EPR signal that significantly influenced the linewidth determination.)

Biophysical characterization: P_{700}

A biophysical analysis was initiated to determine the cause of any functional defects in the mutants. Here we describe a screen for altered properties of P_{700}. It is likely that histidines act as axial ligands to the Chls of P_{700}, as in the purple bacterial RC (Deisenhofer and Michel, 1989), and there is some spectroscopic evidence to this effect (Mac *et al.*, 1996). If so, this screen of the conserved histidines in the last six helices should serve to identify the ones playing this role.

Electron paramagnetic resonance (EPR) spectroscopy was used to study the P_{700}^+ radical cation, which has properties characteristic of an organic cation radical. The *g*-factor of Chl cation radicals in organic solvents is ~2.0026–2.0028 (Lubitz, 1991). P_{700}^+ from WT *C.reinhardtii* has a *g*-factor of 2.0027, similar to that reported previously (Lubitz, 1991). All the mutants investigated had an observable P_{700}^+ EPR signal after illumination at low temperature. None of the mutations caused a change in the *g*-factor.

The linewidth of the P_{700}^+ EPR signal can reveal information about the environment (i.e. hyperfine interactions) experienced by the unpaired electron in P_{700}^+. Typical linewidths for Chl cation radicals are of the order of 0.9 mT (peak to peak), but the linewidth is significantly reduced to 0.70–0.78 mT in P_{700}^+ (Lubitz, 1991 and references therein). None of the double mutants showed a significant change in the P_{700}^+ EPR linewidth (0.75–0.77 mT for all), except for H676Q/H656Q (Table II; Figure 4). The PsaB-H656Q mutation alone also causes a noticeable broadening of the P_{700}^+ EPR linewidth, while the PsaA-H676Q mutation has no detectable effect (Table II). Substitution of leucine for either of the helix 10 histidines causes obvious broadening of the EPR line, similar to that seen in the double-Gln mutant (Table II).

As infrared radiation causes transitions in vibrational states, a $P_{700}^+ - P_{700}$ Fourier transform infrared (FTIR)

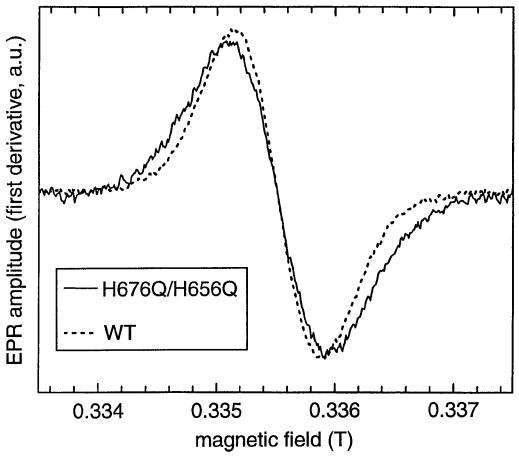

Fig. 4. Nine GHz EPR spectrum of P_{700}^+ in *C.reinhardtii* thylakoid membranes. Thylakoid membranes from *nac2* mutants expressing either WT or H656Q/H676Q PS1 were frozen under illumination (see Materials and methods) and EPR spectra were recorded under the following experimental conditions: microwave power, 0.1 mW; field modulation frequency, 100 kHz; field modulation depth, 0.2 mT; accumulation time, 160 s; temperature, 20 K.

difference spectrum reveals the changes in energies of vibrational transitions caused by the conversion of P_{700} to P_{700}^+, and thus allows access to both the ground state and cation state. Vibrational modes that are sensitive to the photo-oxidation of P700 will give rise to a negative peak corresponding to the energy of the transition in the P_{700} ground state and a positive peak corresponding to that in the P_{700}^+ state. In practice, the most easily observable vibrational modes in Chl are those associated with C=O bonds, such as the 13^1-ketone and 13^2-ester bonds in Chl *a* (Nabedryk, 1996; see Figure 5 for molecular positions). Using modified Chls in organic solvents, the 1715/1700 cm^{-1} and 1753/1748 cm^{-1} peak pairs in the P_{700}^+–P_{700} difference spectrum have been attributed to the 13^1-keto and 13^2-ester carbonyl groups, respectively (Nabedryk *et al.*, 1990; Nabedryk, 1996).

The $P_{700}^+ - P_{700}$ FTIR difference spectra of the mutants are shown in Figure 5. All of the double substitution mutants, except the helix 10 mutant, present FTIR difference spectra similar to that of WT. The H676Q/H656Q mutant displays a clear upshift of 5 cm^{-1} in the 1700 cm^{-1} peak. The PsaA-H676Q mutant displayed a similar shift, whereas the PsaB-H656Q mutant displayed a negligible shift (<1 cm^{-1}; Figure 5). Thus, this change in the 1700 cm^{-1} peak seen in the helix 10 double-Gln mutant can be assigned to the mutation in the PsaA protein. Differences in the spectra seen in the 1630–1660 cm^{-1} region are difficult to attribute, as this congested region contains contributions from peptide C=O bonds as well as water.

The double mutants were also characterized in terms of the P_{700} visible difference spectrum. The 600–750 nm region of the spectrum probes electronic transitions in cofactors such as chlorophylls. Thylakoid membranes from all of the double mutants were examined using a Fourier transform spectrophotometer. Using this method, one can primarily see the main bleaching band due to the oxidation of P_{700}. The position of this band was essentially unchanged in all of the mutants, except for a slight blue-shift seen in the helix 10 double mutant (data not shown).

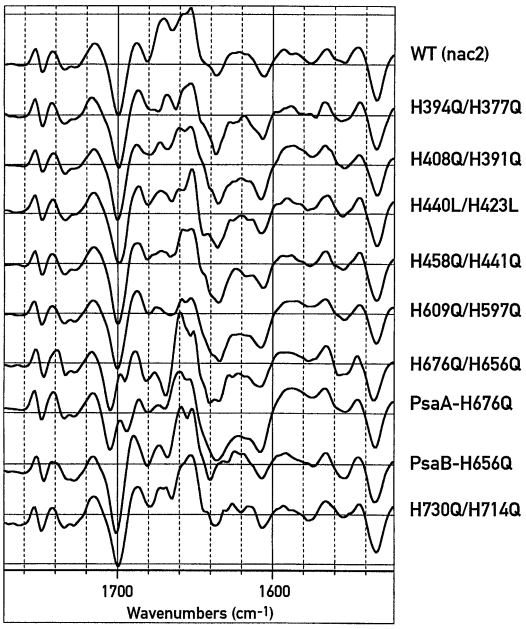

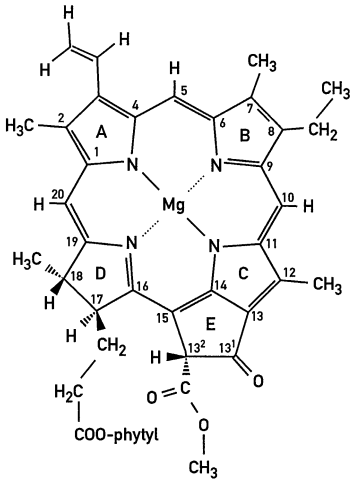

Fig. 5. Light-induced FTIR difference spectra in the 1500 to 1800 cm^{-1} frequency range for the thylakoids of WT and PS1 mutants. Spectral resolution was 4 cm^{-1}. Spectra are the average of 70 000 to 160 000 interferograms. Spectra were normalized for comparable amplitudes of the negative band at 1532 cm^{-1}. The distance between the horizontal grid lines represents 2×10^{-4} absorbance units for the WT spectrum. Beneath the spectra is the structure of Chl *a* using the IUPAC numbering system.

This indicates that the optical properties of P_{700} have not been altered by mutations in helices 6, 7, 9 or 11. Previously, Cui *et al.* (1995) reported that mutations of the conserved histidines in helix 8 of PsaB had a similar lack of effect. As the visible difference spectrum of the H676Q/H656Q mutant was difficult to observe in thylakoid membranes under steady-state conditions, it was necessary to prepare PS1 particles from it and use a laser-flash protocol. Figure 6 presents the spectra obtained in this manner from WT and H676Q/H656Q PS1 particles. Compared with WT, there is a significant blue-shift of the maximal bleaching band (from 699.5 to 695 nm) as well as an additional bleaching at ~670 nm in the helix 10 double-Gln mutant.

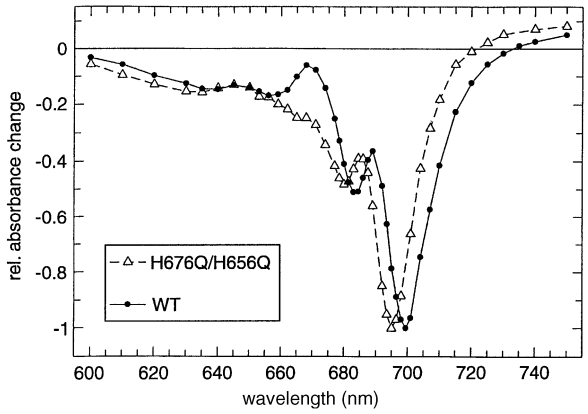

Fig. 6. Visible difference spectra of WT and H676Q/H656Q PS1 particles. Difference spectra were calculated from laser-flash kinetic spectroscopy of PS1 particles prepared from *nac2* mutants expressing either WT or H656Q/H676Q PS1 (see Materials and methods). The spectra are normalized to the same maximal bleaching.

Discussion

We have identified a set of sites in the homologous PsaA/B proteins that are always occupied by histidine. A biophysical analysis of double substitution mutants at all seven sites uniquely identified the site in helix 10 as changing the properties of P_{700} when mutated. In fact, none of the other six double mutations elicited any significant change in the spectra of P_{700}^+ obtained by three very different types of spectroscopy (EPR, FTIR and visible), while the H676Q/H656Q double mutant displayed changes in the properties of P_{700} by all three methods. From this, we conclude that the histidines of helix 10 are uniquely involved in contributing to the environment of the P_{700} chlorophylls.

Role of the helix 10 histidines

One possibility is that the imidazole rings are near the P_{700} chlorophyll macrocycles, and contribute to the hydrophobic environment around them. However, the more drastic effects of substitution with leucine as compared with glutamine argues against this. Histidines can donate and accept hydrogen bonds and are also involved in acid/base chemistry in many enzymes. However, the latter does not occur during P_{700} photochemical events. An inspection of the Chl *a* molecule presents three possibilities for specific interactions with the histidine imidazole ring: as a hydrogen bond donor to the oxygen of the 13^1-keto group; as a hydrogen bond donor to the oxygen of the 13^2-methyl ester; or as the fifth (axial) ligand to the central Mg^{2+}. For reasons discussed below, we favour the last possibility.

The primary reason for favouring the hypothesis that the helix 10 histidines serve as the axial ligands to the P_{700} chlorophylls is that these are the only ones whose mutation affects P_{700} properties. We did not analyse the conserved histidines in helix 8 for changes in P_{700}, as substitution mutants in these sites had no observable effect upon P_{700} (Cui *et al.*, 1995). In addition, two mutations in helix 10 of PsaB, PsaB-H656N and PsaB-H656S, have been reported to produce changes in the P_{700} visible difference and ^{1}H ENDOR spectra (Webber *et al.*, 1996). Thus, all conserved histidines of the last six transmembrane helices of PsaA/B have been mutated, with mutations in helix 10 being the only ones to produce changes in P_{700}. Although residues other than histidine can serve as axial ligands to Chl and BChl (Coleman and Youvan, 1990; Kuhlbrandt and Wang, 1991), there may be reasons why histidine is preferred as the axial ligand to special pair chlorophylls. The histidines that serve this role in the purple bacterial RC are in the fourth transmembrane α-helices of the L and M subunits and are conserved in all Proteobacterial RCs as well as in PS2 (Deisenhofer and Michel, 1989). Moreover, ENDOR and electron spin echo envelope modulation experiments with ^{15}N-labelled PS1 have been interpreted as providing direct proof that histidines serve as the axial ligands to the P_{700} chlorophylls (Mac *et al.*, 1996). If the axial ligands are histidines, then we are driven to the conclusion that they are the helix 10 histidines.

It has been suggested that the PsaA/B proteins represent a fusion between a six-helix 'antenna' Chl-binding protein at the N-terminus and a five-helix RC protein at the C-terminus (Nitschke and Rutherford, 1991; Vermaas, 1994; Fromme, 1996; Nitschke *et al.*, 1996; Rutherford and Nitschke, 1996). The structural model of PS1 at 4 Å resolution lends strong support to this idea (Krauss *et al.*, 1996), as it is now possible to trace the polypeptide backbone from helix 8 to helix 11. The 'antenna–RC fusion' hypothesis makes the prediction that the fourth transmembrane helix of the RC section of PS1 (i.e. helix 10) would be responsible for axial ligation of the P_{700} special pair. Finally, we note that the helix 10 histidines are conserved in the RC proteins of *Chlorobium* and *Heliobacillus* (see Figure 1A), giving credence to the idea that the admittedly low sequence similarity between these three sets of proteins reflects a similar topological and functional structure among the type 1 RCs.

Biophysical properties of helix 10 histidine substitution mutants

Only the mutants in helix 10 exhibited changes in the P_{700}^+ EPR signal. The single substitution mutant PsaB-H656Q exhibits noticeable linewidth broadening, while the corresponding mutation in PsaA (H676Q) does not. As the spin density distribution in P_{700}^+ has been found to be highly asymmetric, with ~85% of the spin on one of the chlorophylls (Käß, 1995; Käß and Lubitz, 1996), mutations that perturb this chlorophyll would be expected to have a much bigger effect upon the magnitude of the hyperfine couplings, and thus upon the EPR linewidth, than those on the other side. If this holds true for the glutamine substitution mutants, then we can assign PsaB-His656 to the dimer half of P_{700} containing most of the spin, and PsaA-His676 with the dimer half of P_{700} harbouring the smaller portion of the spin. An ENDOR analysis of helix 10 mutants is consistent with our proposal above, as somewhat smaller increases (~10%) in the methyl group 12 hyperfine coupling are observed in PsaB-H656Q, but not in PsaA-H676Q (L.Krabben, A.Webber and W.Lubitz, personal communication).

The FTIR difference spectrum of the PsaA-H676Q mutant displays a 4–5 cm^{-1} upshift of the major negative peak at 1700 cm^{-1}, which has been attributed to the vibration of the 13^1-keto group in the ground state (Nabedryk *et al.*, 1990). The positive peak at 1716 cm^{-1},

which has been assigned to the 13^1-keto group in the P_{700}^+ state, is only shifted by 1 cm^{-1}, indicating that the PsaA-H676Q mutation exerts its effect upon this group primarily in the ground state. It is not yet clear which band would correspond to the 13^1-keto group of the Chl on the PsaB side. It may be that this band is located in the congested region of the spectrum (1630–1660 cm^{-1}) containing overlapping contributions of peptide carbonyls and water, which would explain PsaB-H656Q's apparent lack of effect upon the 13^1-keto vibration. We noted a small (1 cm^{-1}) downshift of the differential feature at 1753/1749 cm^{-1}, which has been tentatively attributed to the 13^2-methyl ester carbonyl (Nabedryk, 1996), in both the H676Q/H656Q and PsaB-H656Q mutants, but not in the PsaA-H676Q mutant.

The upshift in stretching frequency of the 13^1-keto group upon change of PsaA-His to Gln might seem, at first glance, to be consistent with the loss of a hydrogen bond to the C=O group. Mutations designed to introduce hydrogen bonds to this keto group in the purple bacterial RC special pair resulted in downshifts of the stretching frequencies by 19–35 cm^{-1} (Nabedryk *et al.*, 1993). However, the frequency of 1700 cm^{-1} is very close to that of Chl *a* in apolar solvent (Nabedryk *et al.*, 1990) and is indicative of a non-hydrogen-bonded 13^1-keto group. Thus, although PsaA-H676Q clearly has an effect upon the P_{700}–P_{700}^+ FTIR spectrum, these effects are not consistent with the gain or loss of a hydrogen bond.

The flash-induced $P_{700}^+ - P_{700}$ visible difference spectrum of the H676Q/H656Q mutant presents two significant changes: a 4–5 nm blue-shift of the main bleaching band and an additional bleaching at ~670 nm (Figure 6). We should note that our WT spectrum deviates from the WT *C.reinhardtii* spectrum measured by Webber *et al.* (1996), where the main bleaching band was centred at 696 nm and had an amplitude ~4-fold that of the proximal bleaching band (at 680–685 nm). It is not clear whether these differences are due to different preparations or to the use of 'wild types' from different genetic backgrounds. Although we observed some variation of the position of the main bleaching band and the relative magnitude of the proximal bleaching band among WT PS1 particles isolated from different *C.reinhardtii* strains, no significant deviations were evident at ~670 nm. An even more pronounced bleaching at ~670 nm was observed for the PsaB-H656N mutant (Webber *et al.*, 1996). This mutant also has a significantly larger 670 nm bleaching than does the PsaB-H656Q single mutant, and PsaA-H676Q has almost no effect upon this region of the spectrum (L.Krabben, E.Schlodder and W.Lubitz, personal communication). The origin of an ~670 nm band has been discussed in terms of excitonic interactions in P_{700} by Breton (1997). It has been suggested that mutation of PsaB-His656 could change the exciton interaction in P_{700} and lead to the appearance of a high-energy exciton component at 670 nm (Webber *et al.*, 1996; Melkozernov *et al.*, 1997).

The hypothesis that the helix 10 histidines are the axial ligands to the Chls of P_{700} makes a strong prediction that the leucine substitution mutants should result in a profound change in P_{700} character. Replacement of either of the axial histidines in the purple bacterial RC special pair to leucine resulted in the conversion of the corresponding BChl to a bacteriopheophytin (i.e. loss of the central Mg^{2+}), and the creation of a new kind of primary donor, the so-called 'heterodimer' special pair (Bylina and Youvan, 1988; Bylina *et al.*, 1990). The EPR signal of the oxidized primary donor in the purple bacterial heterodimer RC displayed linewidth broadening (Bylina *et al.*, 1990; Huber *et al.*, 1996). This was interpreted as a shift from the situation in the WT special pair, where the spin density is ~65% on the L-side (Rautter *et al.*, 1994), to a situation where the spin density is primarily on the remaining BChl (Bylina *et al.*, 1990). The fact that the P_{700}^+ EPR signals are much broader in PsaA-H676L and PsaB-H656L (Table II) would seem to be consistent with the idea that these mutants harbour a 'heterodimer P_{700}'. However, the asymmetry in spin density between the two Chls in P_{700}^+ is already thought to be high (Käß, 1995; Käß and Lubitz, 1996). Further analysis of the PsaB-H656L mutant, including ENDOR spectroscopy of P_{700}^+ and EPR analysis of the $^3P_{700}$ triplet state, will be necessary, but preliminary visible and FTIR spectroscopic results already indicate that P_{700} is strongly disturbed in this mutant (data not shown).

Role of the other conserved histidines

It is interesting that the mutations with the largest effects upon accumulation of PS1 are of residues that are conserved between PS1 and the other type 1 RCs (Figure 1A): the two histidines of helix 6 and the histidine of helix 10 (see Figure 2). We speculate that all of these histidines are playing an important structural role, and that mutation of them either lessens the efficiency of assembly or increases their rate of degradation. The first histidine of helix 6 is especially interesting in this regard, as the decrease in accumulation is completely attributable to the PsaB side; mutation of the corresponding histidine in PsaA, even to leucine, has no effect (K.Redding and J.-D.Rochaix, unpublished data). On the other hand, the second histidine of helix 6 shows the opposite effect, although it is less dramatic: PsaA-H408Q is accumulated at a much lower level than PsaB-H391Q (K.Redding and J.-D.Rochaix, unpublished results). Helix 6 would not be predicted to be part of the RC part of PS1; we speculate that these two histidines ligate antenna Chls whose position is crucial to the assembly of PS1.

Materials and methods

Plasmids and molecular techniques

Plasmids for the reintroduction of *psaB* and *psaA-3* include flanking sequences to direct homologous recombination, as well as the bacterial *aadA* gene, which is used for selection. These vectors will be described in full in a separate manuscript. Briefly, the *psaB* vectors contain 2.5 kbp of upstream sequence, the entire *psaB* gene, and 2.7 kbp of downstream sequence (including all of the *rbcL* gene); a cassette using the *psbD* promoter and 5′ untranslated region to drive expression of aadA (Nickelsen *et al.*, 1994) was inserted at the *Hin*P1 I site between *psaB* and *trnG* in the same orientation as *psaB*. Likewise, the *psaA-3* vectors contain 2.9 kbp of upstream sequence, 1.7 kbp of downstream sequence, and the *psbD–aadA–rbcL* cassette placed in the antisense orientation at an *Eco*RI site 300 bp downstream of the *psaA* third exon. Silent mutations resulting in unique restriction sites were introduced by a three-stage PCR method (Picard *et al.*, 1994) to create a series of vectors, each of which contains two unique sites spaced 370–460 bp apart. All of these vectors restore phototrophic growth and WT levels of PS1 when reintroduced into the corresponding null mutant (K.Redding and J.-D.Rochaix, unpublished data). The substitution mutations were

introduced by the three-stage PCR method (Picard *et al.*, 1994) using oligonucleotides beyond the restriction sites flanking the desired mutation to amplify the PCR products, which were cloned directly into the corresponding plasmids using these same sites. The mutagenic primers introduced silent mutations for easy detection by restriction analysis; all such mutations were contrived so that they did not change the protein sequence, nor did they result in the use of rare codons. Several independent clones were verified by restriction analysis and sequenced; at least two independent subclones were used for transformation.

Algal strain construction

All strains were derived from a 137c background (Harris, 1989). Sexual crosses were performed as described in Harris (1989). The method of constructing the original *psaA-3*Δ and *psaB*Δ null strains (KRC2 and KRC3, respectively) has been described (Fischer *et al.*, 1996). Using the same technology, we have created *psaA-3*Δ and *psaB*Δ null mutations in the *psbA* deletion mutant FUD7 (Bennoun *et al.*, 1986), resulting in KRC4 and KRC5, respectively. The *psaA-3*Δ *psaB*Δ double mutant (KRC6) was created by deleting *psaA-3* in KRC3. This was then crossed to a *mt*$^-$ *nac2-26* (Kuchka *et al.*, 1989) strain to generate KRC22-4A [*mt*$^-$ *nac2-26* (*psaA-3*Δ *psaB*Δ)].

Plasmids were introduced into the appropriate null mutant strains by particle bombardment (Boynton *et al.*, 1988) followed by selection on spectinomycin-containing medium (Goldschmidt-Clermont, 1991). Several representatives of each mutation were characterized to ensure that the observed phenotypes were due to the point mutation and not to secondary mutations. Vectors containing point mutants in *psaA-3*Δ and *psaB* were introduced into KRC2 and KRC3 for *in vivo* analysis and into KRC4 and KRC5 for biochemical and biophysical analysis. Double mutants were created by simultaneously bombarding KRC6 with a mixture of two plasmids containing mutations in the same site in *psaA-3* and *psaB*. Spectinomycin-resistant transformants were passaged alternately on Tris–acetate–phosphate (TAP) + 500 μg/ml spectinomycin (0.5 μEinstein/m^2/s) and TAP (20–50 μEinstein/m^2/s) to select for double transformants. The logic was that single transformants, still harbouring a deletion in the other gene, would be PS1$^-$ and therefore light-sensitive (Spreitzer and Mets, 1981). Homoplasmicity was assessed by PCR reactions on genomic DNA purified from cells by standard methods (Rochaix *et al.*, 1988). All the double substitution mutants were crossed to KRC22-4A, and *nac2* segregants were identified by fluorescence transient screening (see below).

Growth conditions and in vivo tests

TAP and high-salt minimal media were prepared according to Harris (1989). Algae were grown heterotrophically at 25°C in liquid TAP medium in low light fluences (≤1 μEinstein/m^2/s). Growth tests were initiated by spotting 12 μl of log phase cultures onto agar plates. Anaerobiosis of agar plates was imposed using the bioMérieux (Marcy-l'Etoile, France) Generbag Anaer system according to manufacturer's instructions. The remainder of the cultures were harvested for immunoblot analysis. Fluorescence transient analysis was performed as previously described (Farah *et al.*, 1995), using a laboratory-built video fluorescence imaging system based upon that described by Fenton and Crofts (1990).

Preparation and biochemical characterization of membranes, thylakoids and PS1 particles

Crude membrane fractions were made as described (Ohad *et al.*, 1990). Thylakoids and PS1 particles were prepared as described by Fischer *et al.* (1997). Chlorophyll was calculated as described by Porra *et al.* (1989). Protein was measured by the bicinchoninic acid assay (Pierce Chemical Company). O_2 uptake using methyl viologen as a mediator was performed as described by Takahashi *et al.* (1991), except that DCMU was not added, as all membranes assayed contained no PS2. Immunoblotting was performed using standard protocols (Fischer *et al.*, 1997). The anti-PsaF (Farah *et al.*, 1995), anti-psaD (Fischer *et al.*, 1997) and anti-PsaE (Farah *et al.*, 1995) antisera have been described previously. A rabbit polyclonal antiserum was raised against a recombinant protein containing the N-terminus of PsaA fused to a hexahistidine tag. The fusion gene was made by PCR-amplifying the region corresponding to the first 77 codons of PsaA with primers that introduced *Nco*I sites at both ends, and cloning the amplification product as a *Nco*I fragment into pET-15b (Studier *et al.*, 1990). The fusion protein was expressed in BL21(DE3), isolated as inclusion bodies, purified on SDS gels and injected into New Zealand White rabbits using standard protocols.

EPR spectroscopy

Thylakoid membranes (1–1.5 mg Chl/ml) were put in standard Suprasil quartz EPR tubes (4 mm outer diameter) and frozen to 77 K while under illumination from an 800 W lamp using a 4 cm water filter and a 720 nm cut-off filter. Further illumination at low temperatures (10 K) resulted in no further increase in the P_{700}^+ signal amplitude. X-Band EPR spectra were measured on a Bruker ESP300E spectrometer using a standard rectangular Bruker EPR cavity (ER4102T) equipped with an Oxford ESR900 helium cryostat. The microwave frequency was measured using a Hewlett Packard HP5350B frequency counter. The magnetic field was measured with a Bruker ER035M Gaussmeter. The measured *g*-values were corrected for an offset against a known *g* standard [(α,α′)-diphenyl-β-picryl hydroxyl]. Linewidth numbers were determined by curve fitting, using the SimFonia program (Bruker) with an isotropic *g*-value and a single isotropic linewidth.

Fourier transform spectroscopy: infrared and visible

Thylakoid membranes were resuspended in 20 mM MES pH 6.4, 20 mM sodium ascorbate, and 20 μM methyl viologen (for infrared) or 100 μM phenazine methosulfate (PMS; for visible), centrifuged at 200 000 *g*, and the pellet was squeezed between two CaF_2 windows. Samples for visible spectroscopy had an OD_{685} of ~0.9, and samples for infrared spectroscopy were approximately twice as dense. All measurements were done in a cryostat at 280 K. For steady-state illumination, light from a halogen lamp was passed through heat (<700 nm) and red (>630 nm) filters for a duration of 22 s. An equal number of interferograms were recorded before and during continuous illumination, yielding light-minus-dark difference spectra. These measuring cycles were repeated several hundred times with a 30 s period of darkness between each cycle to ensure return to the ground state. Infrared spectroscopy was performed on a Nicolet 60 SX spectrometer equipped with a MCT-A detector, and visible difference spectroscopy in the 650–800 nm range were carried out on a Bruker IFS 88 spectrometer equipped with a tungsten lamp and a silicon diode detector.

Flash spectroscopy

The PS1 particles were diluted to ~10 μM Chl with a buffer containing 10 mM Tricine pH 8.0, 5 mM sodium ascorbate, and 2–5 μM PMS. Absorption changes due to the photo-oxidation and re-reduction of P_{700} were recorded using a laboratory-built flash spectrophotometer. The continuous measuring light from a 45 W tungsten halogen lamp passed through a monochromator (Jobin Yvon H25) with 1.5 nm bandwidth, a 1×1 cm cuvette containing the sample (2 ml), and a combination of interference and coloured glass filters in front of a photomultiplier (Thorn EMI 9558B). The photomultiplier output was DC-coupled via a low-pass RC filter (τ = 1 ms) to a transient digitizer (Tektronix DSA 602A with 11A33 plug-in amplifier). Excitation flashes (~1 mJ/cm^2 at 532 nm; pulse duration = 300 ps full width at half-maximum) were provided by a frequency-doubled Nd/YAG laser (Quantel YG501-10) at a repetition rate of 2 Hz. Many transients (64–256) were averaged at each wavelength. $P_{700}^+ - P_{700}$ difference spectra were constructed from the initial amplitudes of the absorbance changes, obtained by fitting the averaged transients in the time window from 10 to 300 ms post-excitation to a monoexponential decay ($t_{1/2}$ = 20–50 ms, depending on PMS concentration) and extrapolating back to the time of the flash. This procedure eliminates a fluorescence artefact that was present during the first few milliseconds after the flash.

Acknowledgements

The authors wish to thank Nicolas Roggli for preparation of figures, Nicolas Fischer and Michael Hippler for preparation of WT PS1, and Eliane Nabedryk for discussion of FTIR data. K.R. gratefully acknowledges an NSF Plant Biology Fellowship for financial support. F.M. acknowledges a European Union Training and Mobility of Researcher personal fellowship grant. This work was supported by grants from the Human Frontier Science Program and by Grant 31.34014.92 from the Swiss National Foundation.

References

Bendall,D.S. and Manasse,R.S. (1995) Cyclic photophosphorylation and electron transport. *Biochim. Biophys. Acta*, **1229**, 23–38.

Bennoun,P. and Chua,N.H. (1976) Methods for the detection and characterization of photosynthetic mutants in *Chlamydomonas reinhardtii*. In Bücher,T., Neupert,W., Sebald,W. and Werner,S. (eds),

Genetics and Biogenesis of Chloroplasts and Mitochondria. North-Holland Publishing Company, Amsterdam, pp. 33–39.

Bennoun,P., Spierer-Herz,M., Erickson,J., Girard-Bascou,J., Pierre,Y., Delosme,M. and Rochaix,J.-D. (1986) Characterization of Photosystem II mutants of *Chlamydomonas reinhardtii* lacking the *psbA* gene. *Plant Mol. Biol.*, **6**, 151–160.

Boyer,P.D. (1993) The binding change mechanism for ATP synthase – some probabilities and possibilities. *Biochim. Biophys. Acta*, **1140**, 215–250.

Boynton,J.E. *et al*. (1988) Chloroplast transformation in *Chlamydomonas* with high velocity microprojectiles. *Science*, **240**, 1534–1538.

Breton,J. (1977) Dichroism of transient absorbance changes in the red spectral region using oriented chloroplasts II. P-700 absorbance changes. *Biochim. Biophys. Acta*, **459**, 66–75.

Brettel,K. (1997) Electron transfer and arrangement of the redox cofactors in photosystem I. *Biochim. Biophys. Acta*, **1318**, 322–373.

Büttner,M., Xie,D., Nelson,H., Pinther,W., Hauska,G. and Nelson,N. (1992a) Photosynthetic reaction center genes in green sulfur bacteria and in photosystem 1 are related. *Proc. Natl Acad. Sci. USA*, **89**, 8135–8139.

Büttner,M., Xie,D.L., Nelson,H., Pinther,W., Hauska,G. and Nelson,N. (1992b) The photosystem I-like P840-reaction center of green S-bacteria is a homodimer. *Biochim. Biophys. Acta*, **1101**, 154–156.

Bylina,E. and Youvan,D. (1988) Directed mutations affecting spectroscopic and electron transfer properties of the primary donor in the photosynthetic reaction center. *Proc. Natl Acad. Sci. USA*, **85**, 7226–7230.

Bylina,E.J., Kolaczkowski,S.V., Norris,J.R. and Youvan,D.C. (1990) EPR characterization of genetically modified reaction centers of *Rhodobacter capsulatus*. *Biochemistry*, **29**, 6203–6210.

Chitnis,P.R. (1996) Photosystem I. *Plant Physiol.*, **111**, 661–669.

Choquet,Y., Goldschmidt-Clermont,M., Girard-Bascou,J., Kuck,U., Bennoun,P. and Rochaix,J.D. (1988) Mutant phenotypes support a trans-splicing mechanism for the expression of the tripartite *psaA* gene in the *C. reinhardtii* chloroplast. *Cell*, **52**, 903–913.

Chua,N.H. and Bennoun,P. (1975) Thylakoid membrane polypeptides of *Chlamydomonas reinhardtii*: wild-type and mutant strains deficient in photosystem II reaction center. *Proc. Natl Acad. Sci. USA*, **72**, 2175–2179.

Coleman,W.J. and Youvan,D.C. (1990) Spectroscopic analysis of genetically modified photosynthetic reaction centers. *Annu. Rev. Biophys. Biophys. Chem.*, **19**, 333–367.

Cui,L., Bingham,S.E., Kuhn,M., Kass,H., Lubitz,W. and Webber,A.N. (1995) Site-directed mutagenesis of conserved histidines in the helix VIII domain of PsaB impairs assembly of the photosystem I reaction center without altering spectroscopic characteristics of P700. *Biochemistry*, **34**, 1549–1558.

Deisenhofer,J. and Michel,H. (1989) Nobel lecture. The photosynthetic reaction centre from the purple bacterium *Rhodopseudomonas viridis*. *EMBO J.*, **8**, 2149–2170.

Deisenhofer,J., Epp,O., Sinning,I. and Michel,H. (1995) Crystallographic refinement at 2.3 Å resolution and refined model of the photosynthetic reaction centre from *Rhodopseudomonas viridis*. *J. Mol. Biol.*, **246**, 429–457.

Farah,J., Rappaport,F., Choquet,Y., Joliot,P. and Rochaix,J.-D. (1995) Isolation of a psaF-deficient mutant of *Chlamydomonas reinhardtii*: efficient interaction of plastocyanin with the photosystem I reaction center is mediated by the PsaF subunit. *EMBO J.*, **14**, 4976–4984.

Fenton,J.M. and Crofts,A.R. (1990) Computer aided imaging of photosynthetic systems: application of video imaging to the study of fluorescence induction in green plants and photosynthetic bacteria. *Photosyn. Res.*, **26**, 59–66.

Fischer,N., Stampacchia,O., Redding,K. and Rochaix,J.D. (1996) Selectable marker recycling in the chloroplast. *Mol. Gen. Genet.*, **251**, 373–380.

Fischer,N., Setif,P. and Rochaix,J.D. (1997) Targeted mutations in the *psaC* gene of *Chlamydomonas reinhardtii*: preferential reduction of FB at low temperature is not accompanied by altered electron flow from photosystem I to ferredoxin. *Biochemistry*, **36**, 93–102.

Fish,L.E., Kück,U. and Bogorad,L. (1985) Analysis of the two partially homologous P_{700} chlorophyll *a* proteins of maize photosystem I: Predictions based on the primary sequences and features shared by other chlorophyll proteins. *Molecular Biology of the Photosynthetic Apparatus*. Cold Spring Harbor Laboratory Press, New York, pp. 111–120.

Fromme,P. (1996) Structure and function of photosystem I. *Curr. Opin. Struct. Biol.*, **6**, 473–484.

Garnier,J., Guyon,D. and Picaud,A. (1979) Characterization of new strains of nonphotosynthetic mutants of *Chlamydomonas reinhardtii*. I. Fluorescence, photochemical activities, chlorophyll–protein complexes. *Plant Cell Physiol.*, **20**, 1013–1027.

Golbeck,J.H. and Bryant,D.A. (1991) Photosystem I. In Lee,C.P. (ed.), *Current Topics in Bioenergetics: Light-Driven Reactions in Bioenergetics*. Academic Press, New York, Vol. 16, pp. 83–177.

Goldschmidt-Clermont,M. (1991) Transgenic expression of aminoglycoside adenine transferase in the chloroplast: a selectable marker for site-directed transformation of *Chlamydomonas*. *Nucleic Acids Res.*, **19**, 4083–4089.

Hallahan,B.J., Purton,S., Ivison,A., Wright,D. and Evans,M.C.W. (1995) Analysis of the proposed Fe-S_X binding region of Photosystem 1 by site directed mutation of PsaA in *Chlamydomonas reinhardtii*. *Photosyn. Res.*, **46**, 257–264.

Harris,E.H. (1989) *The Chlamydomonas Sourcebook. A Comprehensive Guide to Biology and Laboratory Use*. Academic Press, San Diego.

Hippler,M., Drepper,F., Farah,J. and Rochaix,J.D. (1997) Fast electron transfer from cytochrome c6 and plastocyanin to photosystem I of *Chlamydomonas reinhardtii* requires PsaF. *Biochemistry*, **36**, 6343–6349.

Huber,M., Isaacson,R., Abresch,E., Gaul,D., Schenck,C. and Feher,G. (1996) Electronic structure of the oxidized primary electron donor of the HL(M202) and HL(L173) heterodimer mutants of the photosynthetic bacterium *Rhodobacter sphaeroides*: ENDOR on single crystals of reaction centers. *Biochim. Biophys. Acta*, **1273**, 108–128.

Käß,H. (1995) Die struktur des primären donators P700 in Photosystem I: Untersuchungen mit methoden der stationären und gepulsten elektronsprinresonanz. PhD thesis. Technische Universität Berlin, Germany.

Käß,H. and Lubitz,W. (1996) Evaluation of 2D-ESEEM data of ^{15}N-labeled radical cations of the primary donor P_{700} in Photosystem I and of chlorophyll *a*. *Chem. Phys. Lett.*, **251**, 193–203.

Krauss,N., Schubert,W.D., Klukas,O., Fromme,P., Witt,H.T. and Saenger,W. (1996) Photosystem I at 4 Å resolution represents the first structural model of a joint photosynthetic reaction centre and core antenna system. *Nature Struct. Biol.*, **3**, 965–973.

Kruip,J., Chitnis,P.R., Lagoutte,B., Rogner,M. and Boekema,E.J. (1997) Structural organization of the major subunits in cyanobacterial photosystem 1. Localization of subunits psac, -d, -e, -f, and -j. *J. Biol. Chem.*, **272**, 17061–17069.

Kuchka,M.R., Goldschmidt-Clermont,M., van Dillewijn,J. and Rochaix,J.D. (1989) Mutation at the *Chlamydomonas* nuclear *NAC2* locus specifically affects stability of the chloroplast *psbD* transcript encoding polypeptide D2 of PS II. *Cell*, **58**, 869–876.

Kück,U., Choquet,Y., Schneider,M., Dron,M. and Bennoun,P. (1987) Structural and transcriptional analysis of two homologous genes for the P700 chlorophyll *a*-apoproteins in *Chlamydomonas reinhardtii*: evidence for *in vivo trans*-splicing. *EMBO J.*, **6**, 2185–2192.

Kuhlbrandt,W. and Wang,D.N. (1991) Three-dimensional structure of plant light-harvesting complex determined by electron crystallography. *Nature*, **350**, 130–134.

Liebl,U., Mockensturm-Wilson,M., Trost,J., Brune,D., Blankenship,R. and Vermaas,W. (1993) Single core polypeptide in the reaction center of the photosynthetic bacterium *Heliobacillus mobilis*: structural implications and relations to other photosystems. *Proc. Natl Acad. Sci. USA*, **90**, 7124–7128.

Lubitz,W. (1991) EPR and ENDOR studies of chlorophyll cation and anion radicals. In Scheer,H. (ed.), *Chlorophylls*. CRC Press, Boca Raton, pp. 903–944.

Mac,M., Tang,X.S., Diner,B.A., McCracken,J. and Babcock,G.T. (1996) Identification of histidine as an axial ligand to $P700^+$. *Biochemistry*, **35**, 13288–13293.

Melkozernov,A.N., Su,H., Lin,S., Bingham,S., Webber,A.N. and Blankenship,R.E. (1997) Specific mutation near the primary donor in photosystem I from *Chlamydomonas reinhardtii* alters the trapping time and spectroscopic properties of P700. *Biochemistry*, **36**, 2898–2907.

Nabedryk,E. (1996) Light-induced Fourier transform infrared difference spectroscopy of the primary electron donor in photosynthetic reaction centers. In Mantsch,H. and Chapman,D. (eds), *Infrared Spectroscopy of Biomolecules*. Wily-Liss, New York, pp. 39–81.

Nabedryk,E., Leonhard,M., Mantele,W. and Breton,J. (1990) Fourier transform infrared difference spectroscopy shows no evidence for an enolization of chlorophyll *a* upon cation formation either *in vitro* or during P700 photooxidation. *Biochemistry*, **29**, 3242–3247.

Nabedryk,E., Allen,J.P., Taguchi,A.K., Williams,J.C., Woodbury,N.W. and Breton,J. (1993) Fourier transform infrared study of the primary electron donor in chromatophores of *Rhodobacter sphaeroides* with reaction centers genetically modified at residues M160 and L131. *Biochemistry*, **32**, 13879–13885.

Newman,S.M., Gillham,N.W., Harris,E.H., Johnson,A.M. and Boynton,J.E. (1991) Targeted disruption of chloroplast genes in *Chlamydomonas reinhardtii*. *Mol. Gen. Genet.*, **230**, 65–74.

Nickelsen,J., van Dillewijn,J., Rahire,M. and Rochaix,J.D. (1994) Determinants for stability of the chloroplast *psbD* RNA are located within its short leader region in *Chlamydomonas reinhardtii*. *EMBO J.*, **13**, 3182–3191.

Nitschke,W. and Rutherford,A.W. (1991) Photosynthetic reaction centres: variations on a common structural theme? *Trends Biochem. Sci.*, **16**, 241–245.

Nitschke,W., Mattioli,T. and Rutherford,A.W. (1996) The FeS-type photosystems and the evolution of photosynthetic reaction centers. In Baltscheffsky,H. (ed.), *Origin and Evolution of Biological Energy Conversion*. VCH Publishers, New York, pp. 177–203.

Ohad,I., Adir,N., Koike,H., Kyle,D.J. and Inoue,Y. (1990) Mechanism of photoinhibition *in vivo*. A reversible light-induced conformational change of reaction center II is related to an irreversible modification of the D1 protein. *J. Biol. Chem.*, **265**, 1972–1979.

Picard,V., Ersdal-Badju,E., Lu,A. and Bock,S.C. (1994) A rapid and efficient one-tube PCR-based mutagenesis technique using *Pfu* DNA polymerase. *Nucleic Acids Res.*, **22**, 2587–2591.

Porra,R., Thompson,W. and Kriedemann,P. (1989) Determination of accurate extinction coefficients and simultaneous equations for assaying chlorophylls *a* and *b* with four different solvents: verification of the concentration of chlorophyll standards by atomic absorption spectroscopy. *Biochim. Biophys. Acta*, **975**, 384–394.

Rautter,J., Lendzian,F., Lubitz,W., Wang,S. and Allen,J.P. (1994) Comparative study of reaction centers from photosynthetic purple bacteria: electron paramagnetic resonance and electron nuclear double resonance spectroscopy. *Biochemistry*, **33**, 12077–12084.

Rochaix,J.D. (1992) Post-transcriptional steps in the expression of chloroplast genes. *Annu. Rev. Cell Biol.*, **8**, 1–28.

Rochaix,J.D. (1995) *Chlamydomonas reinhardtii* as the photosynthetic yeast. *Annu. Rev. Genet.*, **29**, 209–230.

Rochaix,J.-D., Mayfield,S., Goldschmidt-Clermont,M. and Erickson,J. (1988) Molecular biology of *Chlamydomonas*. In Shaw,C.H. (ed.), *Plant Molecular Biology: A Practical Approach*. IRL Press, Oxford, pp. 253–275.

Rodday,S.M., Webber,A.N., Bingham,S.E. and Biggins,J. (1995) Evidence that the F_X domain in photosystem I interacts with the subunit PsaC: site-directed changes in PsaB destabilize the subunit interaction in *Chlamydomonas reinhardtii*. *Biochemistry*, **34**, 6328–6334.

Rutherford,A.W. and Nitschke,W. (1996) Photosystem II and the quinone-iron-containing reaction centers: comparisons and evolutionary perspectives. In Baltscheffsky,H. (ed.), *Origin and Evolution of Biological Energy Conversion*. VCH Publishers, New York, pp. 143–175.

Spreitzer,R.J. and Mets,L. (1981) Photosynthesis-deficient mutants of *Chlamydomonas reinhardtii* with associated light-sensitive phenotypes. *Plant Physiol.*, **67**, 565–569.

Studier,W., Rosenberg,A., Dunn,J. and Dubendorff,J. (1990) Use of T7 RNA polymerase to direct expression of cloned genes. *Methods Enzymol.*, **185**, 60–89.

Takahashi,Y., Goldschmidt-Clermont,M., Soen,S.Y., Franzen,L.G. and Rochaix,J.D. (1991) Directed chloroplast transformation in *Chlamydomonas reinhardtii*: insertional inactivation of the psaC gene encoding the iron sulfur protein destabilizes photosystem I. *EMBO J.*, **10**, 2033–2040.

Vallon,O. and Bogorad,L. (1993) Topological study of PSI-A and PSI-B, the large subunits of the photosystem I reaction center. *Eur. J. Biochem.*, **214**, 907–915.

Vermaas,W.F.J. (1994) Evolution in heliobacteria: Implications for photosynthetic reaction center complexes. *Photosyn. Res.*, **41**, 285–294.

Webber,A.N., Gibbs,P.B., Ward,J.B. and Bingham,S.E. (1993) Site-directed mutagenesis of the photosystem I reaction center in chloroplasts. The proline-cysteine motif. *J. Biol. Chem.*, **268**, 12990–12995.

Webber,A.N., Su,H., Bingham,S.E., Kass,H., Krabben,L., Kuhn,M., Jordan,R., Schlodder,E. and Lubitz,W. (1996) Site-directed mutations affecting the spectroscopic characteristics and midpoint potential of the primary donor in photosystem I. *Biochemistry*, **35**, 12857–12863.

Xu,Q., Yu,L., Chitnis,V.P. and Chitnis,P.R. (1994) Function and organization of photosystem I in a cyanobacterial mutant strain that lacks PsaF and PsaJ subunits. *J. Biol. Chem.*, **269**, 3205–3211.

Received August 5, 1997; revised October 13, 1997; accepted October 14, 1997